

Femtosecond dynamics of energy transfer in B800–850 light-harvesting complexes of *Rhodobacter sphaeroides*

(carotenoid/bacteriochlorophyll)

J. K. TRAUTMAN*, A. P. SHREVE*, C. A. VIOLETTE†, HARRY A. FRANK†, T. G. OWENS‡, AND A. C. ALBRECHT*

Department of *Chemistry and †Section of Plant Biology, Cornell University, Ithaca, NY 14853; and ‡Department of Chemistry, University of Connecticut, Storrs, CT 06269

Communicated by Robin M. Hochstrasser, October 13, 1989

ABSTRACT We report femtosecond transient absorption studies of energy transfer dynamics in the B800–850 light-harvesting complex (LHC) of *Rhodobacter sphaeroides* 2.4.1. For complexes solubilized in lauryldimethylamine-*N*-oxide (LDAO), the carotenoid to bacteriochlorophyll (Bchl) B800 and carotenoid to Bchl B850 energy transfer times are 0.34 and 0.20 ps, respectively. The B800 to B850 energy transfer time is 2.5 ps. For complexes treated with lithium dodecyl sulfate (LDS), a carotenoid to B850 energy transfer time of ≤ 0.2 ps is seen, and a portion of the total carotenoid population is decoupled from Bchl. In both LDAO-solubilized and LDS-treated complexes an intensity-dependent picosecond decay component of the excited B850 population is ascribed to excitation annihilation within minimal units of the LHC.

The B800–850 light-harvesting complex (LHC) serves as the principal antenna complex in many purple photosynthetic bacteria (1) and has been extensively studied in *Rhodobacter sphaeroides* and related genera (1–12). The B800–850 LHC contains bacteriochlorophyll (Bchl) and carotenoid pigments in a ratio of 2:1 (2, 3). The Bchl is partitioned between two binding sites; the Q_y absorption of B800 is near 800 nm, that of B850 is near 850 nm. In B800–850 solubilized in lauryldimethylamine-*N*-oxide (LDAO), referred to as B800–850/LDAO, both absorptions are present; in B800–850 treated with lithium dodecyl sulfate (LDS), referred to as B800–850/LDS, the 800-nm absorption is absent (4, 5). Models for the structure of the B800–850 complex suppose the complex to be composed of replications of a minimal pigment-polyptide unit (6, 7). The minimal unit of ref. 6 contains four B850, two B800, and three carotenoid molecules. Two of the carotenoids are coupled only to B850 molecules and the third carotenoid is coupled only to B800 molecules.

Previous work has provided some understanding of singlet energy transfer processes in B800–850 LHCs. In B800–850/LDAO isolated from *Rb. sphaeroides* 2.4.1, total carotenoid to B850 energy transfer efficiency is $95\% \pm 5\%$ (4, 6). At 4 K, 15–25% of the carotenoid excitations are transferred to B800 with subsequent, nearly 100% efficient, B800 to B850 energy transfer; the remaining carotenoid excitations are transferred directly to B850 (8). Measurements of the B800 to B850 transfer have put the time at (i) 1–2 ps at 77 K and < 1 ps at 295 K as determined by picosecond transient absorption spectroscopy (9) and (ii) ≈ 3.3 ps at 4 K as calculated from B800 fluorescence emission measurements (8). For B800–850/LDS the total carotenoid to B850 energy transfer efficiency is only $72\% \pm 3\%$ (4, 6). The dynamics of carotenoid to Bchl energy transfer have been studied by picosecond transient absorption in two strains of *Rhodospseudomonas*

acidophila revealing carotenoid to Bchl transfer times of ≈ 5 ps (10) and ≈ 3 ps (11). The mechanism of carotenoid to Bchl singlet energy transfer is thought to be exchange coupling (13) with transfer occurring from an energetically low-lying carotenoid electronic state analogous to the 2^1A_g state of C_{2h} polyenes (14). The state seen in absorption spectra of carotenoids is likely S_2 , analogous to the 1^1B_u state of C_{2h} polyenes (15). The $S_2 \rightarrow S_1$ internal conversion occurs within 100 fs (16).

MATERIALS AND METHODS

Our femtosecond laser system is similar to that of Gauduel *et al.* (17) and consists of a colliding-pulse modelocked laser (18), a four-stage dye amplifier (19), continuum generation, and a single-stage continuum amplifier. In the present work, the pump pulse was an amplified continuum pulse with ≈ 10 -nm bandwidth centered at 510 nm. Its energy was adjusted between $\approx 0.1 \mu\text{J}$ and $1 \mu\text{J}$ by use of neutral density filters. The probe pulse was an unamplified continuum pulse. The probe wavelength was selected by a monochromator positioned after the sample cell. The partially focused spot sizes of the beams were ≈ 1 mm. The excitation photon flux ($< 10^{15}$ photons/cm² per pulse) was sufficiently low that nonlinear excitation did not contribute to the signals. Pump-probe cross-correlations were typically 240 fs (full width half maximum). Scans were taken with pump and probe polarizations parallel, perpendicular, and at magic angle. Signal amplitudes were polarization dependent even at the highest excitation energies, indicating that the polarization anisotropy created by excitation photoselection was not saturated. In contrast, the energy transfer rates were not polarization dependent; all data reported were taken with parallel polarization. Samples were circulated through a flow system; the sample reservoir was maintained at a temperature of 5–10°C by an ice bath. The concentration of the solutions was adjusted to obtain an optical density of ≈ 0.3 for a 2-mm path length at 510 nm. B800–850/LDAO and B800–850/LDS were prepared from chromatophores of *Rb. sphaeroides* 2.4.1 according to established procedures (4). Energy transfer time constants were determined by fitting the data with a nonlinear least-squares routine to a function given by the convolution of the cross-correlation with the signal expected from a postulated kinetic model.

RESULTS AND DISCUSSION

Our experiments consist of exciting the carotenoid population at time zero and then, using various probe wavelengths, monitoring the time evolution of excited state populations of

B800, B850, and carotenoid molecules. Experimental results with brief discussions are presented according to the preparation (LDS or LDAO) and according to the excited state species probed after carotenoid excitation.

B800 Kinetics in B800–850/LDAO. The transient absorption kinetics of the B800–850/LDAO complex at 800 nm after excitation at 510 nm are shown in Fig. 1. The induced transmission increases quickly and then decays in picoseconds into a small induced absorption, which itself decays on a nanosecond time scale. Our data are well fit to a model consisting of carotenoid to B800 transfer followed by B800 to B850 transfer with contributions to the signal coming from both B800 and B850; at this probe wavelength, the excitation of B800 results in a bleach, the excitation of B850 gives an induced absorption. The induced absorption is attributed to a B850 $S_1 \rightarrow S_n$ transition because the B850 S_1 is the only species created within picoseconds that still exists after hundreds of picoseconds. This is in agreement with a previous assignment (9) in which an induced absorption was found within picoseconds at 800 nm after excitation at 800 nm. A direct fit of the data requires knowing the equation of motion of the excited B850 population. An alternative approach is to “correct” the data by subtracting the B850 contribution using the appropriately scaled transient absorption curve obtained under identical experimental conditions but with the probe wavelength tuned to 850 nm. The response to an 850-nm probe is taken to be a direct measure of the B850 population. Due to the rather complicated B850 kinetics, this procedure, which uses a simple fit function, is preferred. The fit parameters thus obtained are 0.34 ps and 2.5 ps for the carotenoid to B800 and B800 to B850 transfer times, respectively. Their uncertainty is estimated to be approximately $\pm 10\%$.

B850 Kinetics in B800–850/LDAO. Curves for the induced transmission at 850 nm after 510-nm excitation at three different intensities are shown in Fig. 2. Given the results of the 800-nm probe scans and the known carotenoid to B850 and carotenoid to B800 transfer efficiencies (8), a two-component rise in the induced transmission is expected. At the lowest pump intensities used, this is seen. At higher pump intensities, a picosecond absorption recovery component becomes significant. We ascribe this to B850–B850 singlet-singlet annihilation.

A definitive treatment of the picosecond absorption recovery at 850 nm requires precise knowledge of the excitation flux, secure determination of the long time decays, and scans at pump intensities lower than those used here. Nevertheless,

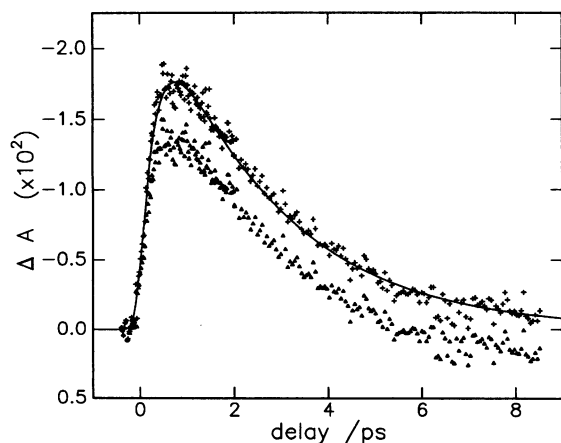


FIG. 1. Induced transmission at 800 nm after excitation at 510 nm in B800–850/LDAO. The lower curve shows the raw data. The upper curve is corrected for B850 S_1 absorption at 800 nm as described in the text. The line through the corrected data is a fit with a rise time of 0.34 ps and a fall time of 2.5 ps.

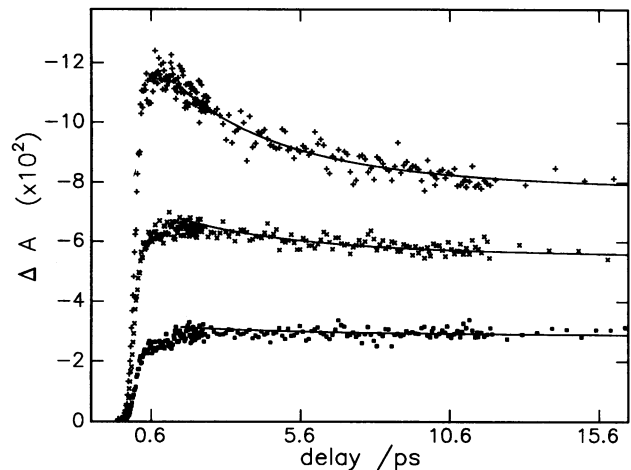


FIG. 2. Induced transmission at 850 nm after excitation at 510 nm in B800–850/LDAO. Fits (—) to the decays are overlaid. The relative excitation intensities for the three curves were 5:2.5:1. The annihilation parameters (see ref. 20) are chosen to fit the highest excitation intensity data for which the average number of excitations per domain $z = 0.9$, the annihilation rate constant $\gamma/2 = 0.125 \text{ ps}^{-1}$, and the monomolecular decay rate constant $k = 0.001 \text{ ps}^{-1}$. For the lower two curves, z is scaled according to the relative excitation intensities; $\gamma/2$ and k are unchanged.

the data can be fit, as shown in Fig. 2, with the standard annihilation theory of Paillotin *et al.* (20). The values of z , the average number of excitations per domain, and the value of $\gamma/2$, the annihilation rate constant, required to fit our data are very different from those previously determined for the B800–850 complexes of *Rb. sphaeroides* (12). However, this is not necessarily a contradiction. Our experiments were performed at the high end of the excitation intensity range used in ref. 12. At these intensities, the probability, P , that a given molecule will be excited by the pump pulse is significant ($P > 0.1$). The values of z from our data, taken with the estimated value of P , imply a domain size on the order of only a few molecules—that is, a domain comparable to the minimal unit of ref. 6. Then a scheme that explains both the present results and those of ref. 12 is the following. For $P \ll 1$, annihilation must occur by excitation transfer between B850s in different minimal units. In this case, the annihilation rate is relatively slow. But, as P is made larger, the probability that the pump pulse creates more than one excitation in a given minimal unit is not negligible. The excitations within a minimal unit are very mobile (hopping times $< 1 \text{ ps}$) and, consequently, the annihilation time constant that dominates the early time dynamics is on the order of picoseconds. Thus, the low and high excitation intensity experiments explore two different domains. To properly fit long time scans taken with high excitation intensity and ultrafast time resolution, a solution to the master equation is needed that takes account of both annihilation channels. The time range of the present experiments is sufficiently short for the slower component not to interfere significantly with the fit of the fast annihilation.

At the lower pump intensity, the data are fit with a two-channel model consisting of the direct carotenoid to B850 transfer and the indirect carotenoid to B800 to B850 transfer. The carotenoid to B800 and B800 to B850 transfer times from the fit to the 800-nm probe data (see *B800 Kinetics in B800–850/LDAO*) are used in the fit of the 850-nm probe scans. A direct carotenoid to B850 transfer time of 0.20 ps is determined. For the fit shown in Fig. 3, the ratio of the amplitudes of the direct channel to the indirect channel is 4:1. This ratio was chosen to match (within experimental uncertainty) that determined from measurements of the excitation

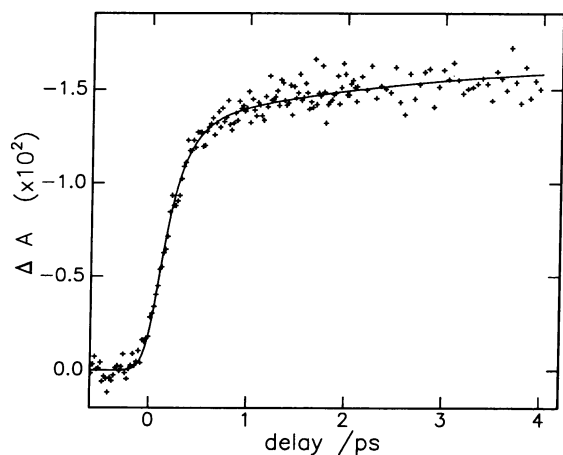


FIG. 3. Induced transmission at 850 nm after excitation at 510 nm in B800-850/LDAO. These are the lowest excitation intensity data taken. The fit (—) is for a two-channel model: a direct channel (carotenoid \rightarrow B850) with a transfer time of 0.20 ps and an indirect channel (carotenoid \rightarrow B800 \rightarrow B850) with transfer times of 0.34 ps and 2.5 ps. The relative amplitudes of the channels are 4:1.

profiles of B800 and B850 fluorescence (8). An independent measure of the ratio is possible from transient absorption data, but the presence of annihilation complicates its determination in this work. If, in the fitting procedure, the ratio is allowed to vary, its value is found to be strongly coupled to the B800 to B850 energy transfer time and both are sensitive to the presence of annihilation. Even though the annihilation model predicts that the maximum signal in the 850-nm data of Fig. 3 is suppressed only slightly (<5%) relative to the hypothetical intraminimal unit annihilation-free result, we are unable to independently determine both the ratio and the B800 to B850 energy transfer time from the 850-nm probe data. However, as shown in Fig. 3, the data are well fit using the B800 to B850 transfer time determined from the 800-nm probe data and a ratio fixed at 4:1. The 0.2-ps carotenoid to B850 energy transfer time is insensitive to the presence of annihilation; an uncertainty of ≈ 50 fs is estimated.

Carotenoid Kinetics in B800-850/LDAO. From the 800- and 850-nm probe data (see *B800 Kinetics in B800-850/LDAO* and *B850 Kinetics in B800-850/LDAO*) and the near 100% carotenoid to Bchl transfer efficiency, one expects that when both the pump and the probe are tuned to the carotenoid absorption region an initial response, indicative of carotenoid excitation and subsequent S_2 to S_1 internal conversion, should be observed. This response should decay in ≈ 250 fs with two components, one for transfer to B850 and one for transfer to B800, but these may not be separately resolvable. This conjecture is not borne out in the data shown in Fig. 4 where the pump wavelength is 510 nm, as before, and the probe wavelength is 520 nm. Instead, the recovery is fit to an $a \rightarrow b \rightarrow c$ scheme in which the a to b transfer time is 0.25 ps and the b to c transfer time is 1.4 ps. Both a and b contribute to the bleach with relative amplitudes of 3.5:1. The initial state, a , is assumed to be created instantaneously. This results in a slight discrepancy between the data and the fit on the rise but doesn't affect the fit of the decay. There is no evidence in the 800- or 850-nm probe data (see *B800 Kinetics in B800-850/LDAO* and *B850 Kinetics in B800-850/LDAO*) for a carotenoid to Bchl transfer of 1.4 ps. Furthermore, the efficiency of carotenoid to Bchl transfer in B800-850/LDAO complexes is $\approx 95\%$, so the picosecond component of the recovery of the 520-nm bleach cannot be assigned to a subset of uncoupled carotenoids.

One interpretation is as follows. The fast a to b process is transfer from electronically excited carotenoids to B800 and B850, with the two components not separately resolved. The

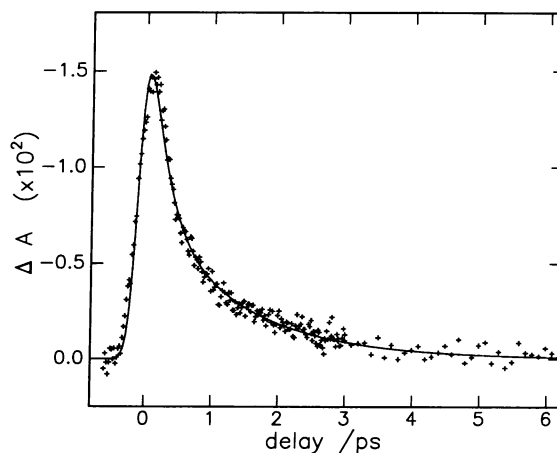


FIG. 4. Induced transmission at 520 nm after excitation at 510 nm in B800-850/LDAO. The fit (—) is for an $a \rightarrow b \rightarrow c$ model representing carotenoid $S_1 \rightarrow S_0^* \rightarrow S_0$ as described in the text. The transfer time, $a \rightarrow b$, is 0.25 ps and the vibrational cooling time, $b \rightarrow c$, is 1.4 ps. The relative contributions of S_1 and S_0^* to the response are 3.5:1.

carotenoids are left in their electronic ground states with distribution of excess vibrational energy that will be narrowly distributed around ≈ 8000 cm^{-1} if the transfer is directly to S_1 of B850. The b to c process represents the equilibration of these "hot" carotenoids with their environment—that is, the vibrational cooling of the carotenoids to their thermalized ground state, c . The cooling rate depends on the internal temperature (21) and the strength of the coupling to the "solvent;" 8000 cm^{-1} of excess vibrational energy in a molecule with 300 normal modes will raise the temperature by perhaps 100 K. A cooling time constant of 1.4 ps is reasonable based on previous studies of large molecules (21-23).

In general, as the vibrational temperature of a molecule increases, the absorption spectrum broadens and flattens (the area being conserved). Near the peak absorption the "hot" - "cold" difference spectrum will be negative, while to the red of the transition origin the difference spectrum will be positive. The data presented in Fig. 4 are for a probe wavelength of 520 nm. A scan with a probe wavelength of 480 nm displays identical kinetics but the relative amplitude of the slow component is approximately twice that of the 520-nm scan (data not shown). The 480-nm light probes near the peak of the $S_0 \rightarrow S_2$ absorption where the hot - cold difference spectrum will be the most negative while a 520-nm probe wavelength is likely near the difference spectrum zero crossing. A study of the evolution of the entire carotenoid spectrum should test this interpretation.

B850 Kinetics in B800-850/LDS. When the B800-850/LDS complex is pumped at 510 nm and probed at 800 nm, a small induced absorption is observed (data not shown). The kinetics of the response are identical to those of the 850-nm probe scan of this complex; the magnitude of the response is comparable to the induced absorption found at long time in the 800-nm probe scan of the B800-850/LDAO complex. The transient signal at 800 nm is thus attributed to B850 $S_1 \rightarrow S_n$ absorption.

Data from 850-nm probe scans taken over a range of excitation intensities are presented in Fig. 5. As in the B800-850/LDAO data, a fast absorption recovery component is found at higher pump intensities. The values of z from the annihilation analysis of this recovery are listed in the figure legend and are comparable to those required to fit B800-850/LDAO data (see *B850 Kinetics in B800-850/LDAO*). However, the annihilation rate constant itself is ≈ 5 times faster in the LDS-treated complexes. The annihilation

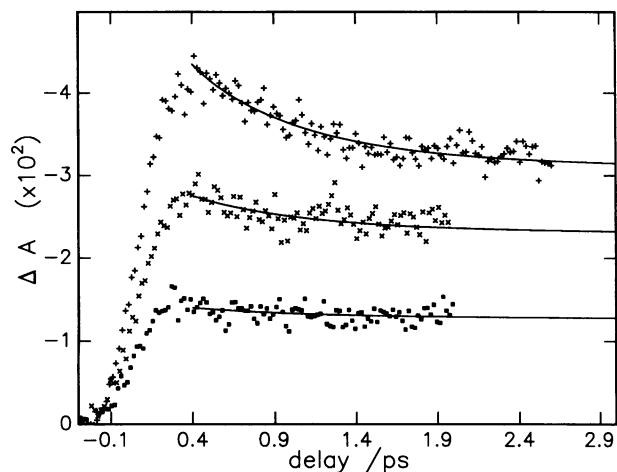


FIG. 5. Induced transmission at 850 nm after excitation at 510 nm in B800-850/LDS. Fits to the decays are overlaid (—). The relative excitation intensities for the three curves were 4:2:1. For the highest excitation intensity data, $z = 0.7$, $\gamma/2 = 0.75 \text{ ps}^{-1}$, and $k = 0.001 \text{ ps}^{-1}$. For the lower two curves z is scaled according to the relative excitation intensities while $\gamma/2$ and k are unchanged. See Fig. 2 for details.

model suggests that the increased annihilation rate is due to an increased excitation hopping rate among B850s within the minimal unit (assuming the probability of annihilation upon encounter is unchanged).

In B800-850/LDS, the carotenoid to B850 transfer time cannot be accurately determined, first, because the transfer rate is fast—i.e., less than the cross-correlation width—and, second, because at the lowest pump intensities used where the fast annihilation interference is reduced to a few percent, the data are quite noisy. The best estimate for the carotenoid to B850 energy transfer time is $\leq 200 \text{ fs}$. Finally, no evidence for a slower component is seen.

Carotenoid Kinetics in B800-850/LDS. The LDS-induced decrease in the carotenoid to B850 energy transfer efficiency (4, 6) can be interpreted in two ways: the transfer rate is slowed sufficiently to cause the overall efficiency to drop by $\approx 25\%$ or $\approx 1/4$ of the carotenoids are decoupled from Bchl while the remaining 3/4 transfer with nearly 100% efficiency. The extremely fast increase in the 850-nm probe data is consistent with the latter explanation. So, when the probe wavelength is tuned to the carotenoid absorption, one ought to find a two-component bleach recovery. The faster component should have an $\approx 200\text{-fs}$ decay, corresponding to energy transfer to B850, the slower component should have the *in vivo* lifetime of the uncoupled carotenoid S_1 state. Their relative amplitudes should be $\approx 3:1$. Furthermore, in accord with the B800-850/LDAO 520-nm probe data (see *Carotenoid Kinetics in B800-850 LDAO*), each of these decays should exhibit two components: one for the transition to the hot electronic ground state and one for the subsequent vibrational cooling. Finally, after $S_1 \rightarrow S_0$ internal conversion an uncoupled carotenoid ought to be hotter, and therefore cool more slowly, than a carotenoid that has transferred electronic energy to a B850.

It is unrealistic to attempt to fit our data to this model containing seven parameters. Instead, reasonable parameters are used (chosen, when possible, to match values determined above). Specifically, the coupled carotenoids are assigned a transfer time of 0.2 ps and a cooling time of 1.3 ps; the uncoupled carotenoids are assigned an internal conversion time of 4 ps and a 2-ps cooling time. The relative amplitudes of the two channels are taken to be 3:1. The populations of S_1 and of hot S_0 are taken to contribute to the transient absorption response in a ratio of 2:1 for both

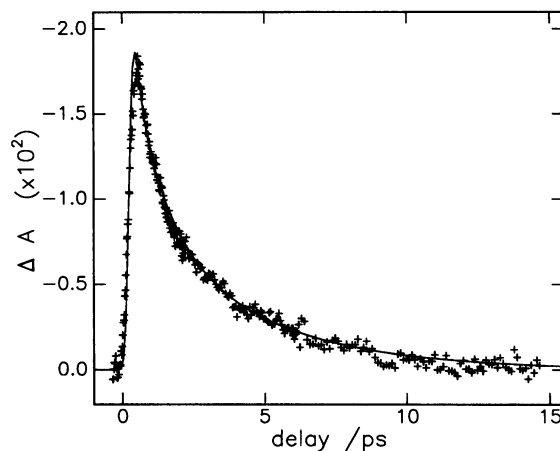


FIG. 6. Induced transmission at 480 nm after excitation at 510 nm in B800-850/LDS. The fit is described in the text.

coupled and uncoupled carotenoids. The data for a probe wavelength of 480 nm, with a fit, are shown in Fig. 6. Of course, the good fit achieved using these parameters does not demonstrate their uniqueness.

CONCLUSIONS

In summary, we report several energy transfer times in LHCs of *Rb. sphaeroides* 2.4.1. In B800-850/LDAO complexes, the carotenoid to B850 transfer time is 0.20 ps, the carotenoid to B800 transfer time is 0.34 ps, and the B800 to B850 transfer time is 2.5 ps. In the B800-850/LDS complexes, the carotenoid to B850 transfer time is $\leq 0.2 \text{ ps}$.

The similarity of carotenoid to B850 energy transfer times in B800-850/LDS and B800-850/LDAO together with the existence of a subpopulation of carotenoids having a longer-lived excited state in the LDS-treated complexes make evident that the overall decrease in carotenoid to B850 energy transfer efficiency in the LDS-treated complexes (4, 6) is a result of the decoupling of a subpopulation of the carotenoids from Bchl. These likely are those carotenoids that are coupled to B800 in B800-850/LDAO. Although the ratio of carotenoids that are directly coupled to B850 to those coupled to B800 isn't independently determined in this work, our data are more consistent with previous fluorescence quantum yield results (4, 6) than with the 2:1 ratio used in the model of Kramer *et al.* (6).

The principal objective of this work has been to determine the carotenoid to Bchl energy transfer times in these LHCs. However, interesting annihilation effects have also been discovered on a heretofore unexplored time scale, possibly involving annihilation within the minimal unit. Further annihilation experiments on an ultrafast time scale ought to provide detailed information concerning the coupling within the B800-850 minimal unit. At the very least, such studies should be able to determine the number of coupled chromophores in such a structure.

Support for this work is gratefully acknowledged: A.C.A. thanks the National Science Foundation (Grant CHE-8617960), the National Institutes of Health (Grant GM-10865), and the Cornell Materials Science Center; H.A.F. thanks the National Institutes of Health (Grant GM-30353) and the U.S. Department of Agriculture Competitive Research Grant Office (Grant 88-37130-3938); and T.G.O. thanks the National Science Foundation (Grant DMB-8803626).

1. Zuber, H. (1985) *Photochem. Photobiol.* **42**, 821-844.
2. Radcliffe, C. W., Pennoyer, J. D., Broglie, R. M. & Niederman, R. A. (1984) in *Advances in Photosynthesis Research*, ed.

- Sybesma, C. (Nijhoff, The Hague, Netherlands), Vol. 2, pp. 215–220.
3. Evans, M. B., Cogdell, R. J. & Britton, G. (1988) *Biochim. Biophys. Acta* **935**, 292–298.
4. Chadwick, B. W., Zhang, C., Cogdell, R. J. & Frank, H. A. (1987) *Biochim. Biophys. Acta* **893**, 444–451.
5. Clayton, R. K. & Clayton, B. J. (1981) *Proc. Natl. Acad. Sci. USA* **78**, 5583–5587.
6. Kramer, H. J. M., van Grondelle, R., Hunter, C. N., Westerhuis, W. H. J. & Ames, J. (1984) *Biochim. Biophys. Acta* **765**, 156–165.
7. Scherz, A. & Parson, W. W. (1986) *Photosyn. Res.* **9**, 21–32.
8. van Grondelle, R., Kramer, H. J. M. & Rijgersberg, C. P. (1982) *Biochim. Biophys. Acta* **682**, 208–215.
9. Bergström, H., Sundström, V., van Grondelle, R., Gillbro, T. & Cogdell, R. (1988) *Biochim. Biophys. Acta* **936**, 90–98.
10. Wasielewski, M. R., Tiede, D. M. & Frank, H. A. (1986) in *Ultrafast Phenomena V*, Springer Series in Chemical Physics, eds. Fleming, G. R. & Siegman, A. E. (Springer, Berlin), Vol. 46, pp. 388–392.
11. Gillbro, T., Cogdell, R. J. & Sundström, V. (1988) *FEBS Lett.* **235**, 169–172.
12. van Grondelle, R., Hunter, C. N., Bakker, J. G. C. & Kramer, H. J. M. (1983) *Biochim. Biophys. Acta* **723**, 30–36.
13. Dexter, D. L. (1953) *J. Chem. Phys.* **21**, 836–850.
14. Cogdell, R. J. & Frank, H. A. (1987) *Biochim. Biophys. Acta* **895**, 63–79.
15. Wasielewski, M. R. & Kispert, L. D. (1986) *Chem. Phys. Lett.* **128**, 238–243.
16. Bondarev, S. L., Dvornikov, S. S. & Bachilo, S. M. (1988) *Opt. Spectrosc. (USSR)* **64**, 268–270.
17. Gauduel, Y., Migus, A., Martin, J. L., Lecarpentier, Y. & Antonetti, A. (1985) *Ber. Bunsenges. Phys. Chem.* **89**, 218–222.
18. Valdmanis, J. A., Fork, R. L. & Gordon, J. P. (1985) *Opt. Lett.* **10**, 131–133.
19. Fork, R. L., Shank, C. V. & Yen, R. (1982) *Appl. Phys. Lett.* **41**, 223–225.
20. Paillotin, G., Swenberg, C. E., Breton, J. & Geacintov, N. E. (1979) *Biophys. J.* **25**, 513–534.
21. Laermer, F., Elsaesser, T. & Kaiser, W. (1989) *Chem. Phys. Lett.* **156**, 381–386.
22. Kaiser, W. & Seilmeier, A. (1987) *Ber. Bunsenges. Phys. Chem.* **91**, 1201–1205.
23. Henry, E. R., Eaton, W. A. & Hochstrasser, R. M. (1986) *Proc. Natl. Acad. Sci. USA* **83**, 8982–8986.